

This work is on a Creative Commons Attribution 4.0 International (CC BY 4.0) license, <https://creativecommons.org/licenses/by/4.0/>. Access to this work was provided by the University of Maryland, Baltimore County (UMBC) ScholarWorks@UMBC digital repository on the Maryland Shared Open Access (MD-SOAR) platform.

Please provide feedback Please support the ScholarWorks@UMBC repository by emailing scholarworks-group@umbc.edu and telling us what having access to this work means to you and why it's important to you. Thank you.

Striatal RGS7 regulates depression-related behaviors and stress-induced reinstatement of cocaine conditioned place preference

<https://doi.org/10.1523/ENEURO.0365-20.2020>

Cite as: eNeuro 2021; 10.1523/ENEURO.0365-20.2020

Received: 16 August 2020

Revised: 22 November 2020

Accepted: 24 November 2020

This Early Release article has been peer-reviewed and accepted, but has not been through the composition and copyediting processes. The final version may differ slightly in style or formatting and will contain links to any extended data.

Alerts: Sign up at www.eneuro.org/alerts to receive customized email alerts when the fully formatted version of this article is published.

Copyright © 2021 Sutton et al.

This is an open-access article distributed under the terms of the Creative Commons Attribution 4.0 International license, which permits unrestricted use, distribution and reproduction in any medium provided that the original work is properly attributed.

1 **Striatal RGS7 regulates depression-related behaviors and stress-induced reinstatement of**
2 **cocaine conditioned place preference**

3 Abbreviated title: Rgs7 and stress-induced reinstatement

4
5 Laurie P. Sutton^{1,2}, Natalia Khalatyan³, Jeffrey N. Savas³ and Kirill A. Martemyanov¹

6
7 1 Department of Neuroscience, The Scripps Research Institute, Jupiter, FL 33458 USA

8 2 Present address: Department of Biological Sciences, University of Maryland Baltimore
9 County, Baltimore, MD 21250 USA

10 3 Department of Neurology, Northwestern University Feinberg School of Medicine, Chicago, IL
11 USA

12
13 Author Contributions: LPS, JNS, KAM Designed Research; LPS and KAM Wrote the paper; NK
14 and LPS Performed Research and Analyzed data.

15
16 Correspondence should be addressed to Laurie P. Sutton at suttonl@umbc.edu

17
18 Number of Figures: 5

19 Number of Tables: 0

20 Number of Multimedia: 0

21 Number of words for Abstract: 222

22 Number of words for Significance Statement: 85

23 Number of words for Introduction: 458

24 Number of words for Discussion: 1259

25
26 Acknowledgements: We thank Ms. Natalia Martemyanova for producing and maintaining mice
27 used in this study.

28
29 Conflict of Interest: Authors report no conflict of interest.

30
31 Funding Source: NIH grant DA036596 and MH105482 (to KAM)

36 **ABSTRACT**

37 The striatum plays a key role in both reward-related and affective behaviors and disruptions to
38 this circuit contributes to depression and drug addiction. However, our understanding of the
39 molecular factors that facilitate and modify these processes are incomplete. Striatal function is
40 modulated by G protein coupled receptors (GPCRs) that process vast neuromodulatory inputs.
41 GPCR signaling is negatively regulated by Regulator of G protein Signaling (Rgs) proteins. In
42 this study, we examine the role of striatal Rgs proteins in depressive-like and reward-related
43 behaviors in male mice. Using a genetic mouse model with specific elimination of Rgs7 in
44 striatal neurons we found that these mice exhibit an anxiolytic-like and antidepressant-like
45 phenotype. In contrast, knockout of Rgs9, an abundant Rgs protein in the same neuronal
46 population did not affect the behavioral outcome in the depressive-like tests. Mice lacking
47 striatal Rgs7 did not show significant differences in cocaine-induced psychomotor activation,
48 sensitization or conditional place preference (CPP). Interestingly, loss of Rgs7 in the striatum
49 made mice resilient to stress-induced but not drug-induced reinstatement of cocaine CPP.
50 Analysis of striatal proteome revealed that loss of Rgs7 selectively affected expression of several
51 networks, most prominently including proteins involved in translation and vesicular exocytosis.
52 Together, these findings begin to demonstrate the specific contribution of Rgs7 acting in the
53 striatum towards depression as it relates to stress-induced reinstatement of drug use.

54

55 **SIGNIFICANCE STATEMENT**

56 G protein coupled receptors (GPCRs) play a key role in modulating responses of striatal neurons
57 that ultimately shape complex behaviors such as mood and reward. The extent of GPCR
58 signaling is tightly controlled by Regulators of G protein signaling (Rgs). In this study, we report
59 a key role of Rgs7 in the striatum towards depression and reward-related behaviors, while
60 addressing the effects of stress on these behavioral outcomes. Together our findings provide new
61 insights into the molecular mechanisms involved in stress induced drug seeking behaviors.

62

63

64 INTRODUCTION

65 Converging human and rodent findings demonstrate a key role for the striatum in
66 processing and responding to rewarding and aversive stimuli and is a critical mediator of
67 affective states (Berton et al., 2006; Lobo and Nestler, 2011). The striatum serves as a central
68 interface for integrating information from the ventral tegmental area (VTA) and prefrontal cortex
69 (PFC) onto medium spiny neurons (MSNs). These afferent inputs onto MSNs lead to long-term
70 adaptations in dendritic spine density, neuronal excitability and changes in gene expression
71 which drive emotional and rewarding processes (Cerovic et al., 2013; Nelson and Kreitzer,
72 2014). Dysregulation of the striatal circuit contribute to several neuropsychiatric disorders
73 including mood disorders and drug addiction (Lobo and Nestler, 2011; Francis and Lobo, 2017).
74 Mood disorders have a high comorbidity with drug addiction which may stem from common
75 molecular mechanisms (Pettinati et al., 2013). However, despite the relevance of the striatum in
76 mediating reward and mood behaviors, we are just beginning to understand the neuroadaptations
77 within the striatum that contribute to these neuropsychiatric disorders.

78 The activity of MSNs is controlled by multiple neurotransmitters, many of which act on
79 their cognate G protein coupled receptor (GPCRs) to drive striatal-mediated behaviors (Kreitzer,
80 2009; Johnson and Lovinger, 2016). Activated GPCRs promote dissociation of the G protein
81 heterotrimer into $G\beta\gamma$ and the $G\alpha$ -GTP subunits which trigger various cellular responses. To
82 control the strength and duration of this signaling, Regulator of G protein signaling (RGS)
83 proteins accelerate the inactivation of the $G\alpha$ subunit promoting heterotrimer reformation (Ross
84 and Wilkie, 2000; Hollinger and Hepler, 2002). In particular, a member of the RGS family, Rgs7
85 has been shown to play key roles in suppressing $G_{\alpha i/o}$ -mediated signaling via dopamine, opioid
86 and adrenergic GPCRs thereby controlling mood and reward processes (Masuho et al., 2013;
87 Sutton et al., 2016; Orlandi et al., 2019). Mice with a global knockout of Rgs7 exhibit marked

antidepressant-like behaviors and a resilience to chronic stress-induced depression (Orlandi et al., 2019). This phenotype can be suppressed by re-expression of *Rgs7* within the PFC implicating this brain region in the effects. However, it remained unclear whether other neuronal populations and brain structures are involved in the effects of *Rgs7* on affective behaviors in particular as it relates to addiction. In the striatum, *Rgs7* has been implicated in dictating the sensitivity of mice to rewarding and reinforcing effects of morphine (Sutton et al., 2016). In this study we explore the role of striatal *Rgs7* in depression related phenotypes and its relevance to regulating reward-related behaviors. We report that inactivation of *Rgs7* specifically in striatal neurons results in prominent antidepressant-like effects and protects male mice from stress-induced but not drug-cued reinstatement of cocaine conditional place preference. Analysis of molecular changes suggest the involvement of complex gene networks in the observed phenotypes.

100

101 **METHODS**

102 **Animals**

All studies were carried out in accordance with the National Institute of Health guidelines and were granted formal approval by the Institutional Animal Care and Use Committee. Conditional knockout mice were generated by crossing homozygous *Rgs7^{loxP/loxP}* with heterozygous *Rgs9^{cre}* mice to generate *Rgs7^{loxP/loxP}Rgs9^{cre}* knockout mice and their wild-type littermate control mice, *Rgs7^{loxP/loxP}* (Dang et al., 2006; Cao et al., 2012). Generation of *Rgs9^{-/-}* (Witherow et al., 2000) mice have been previously described. Mice were housed in groups on a 12-h light-dark cycle (lights on at 7:00 a.m.) with food and water available ad libitum. We relied exclusively on

109

littermates for all the comparisons. Male mice were used in all the behavioral and biochemical assays and were between the ages of 2-4 months.

Behavioral Paradigms

Marble Burying: Marble burying (MB) was conducted in a homecage-like environment (27x16.5x12.5 cm) with 5 cm corn cob bedding. 20 glass marbles were overlaid in a 4x5 equidistant arrangement and testing consisted of a 30min exploration period. The number of marbles that were at least two-thirds buried at the end of the trial were counted as buried.

Elevated Plus Maze: The elevated plus maze was performed using a black, plexiglass elevated plus maze (Med Associates, St. Albans, VT). Lighting for the maze was set at 200 lux in the center of the plus maze, 270 lux on the open arms, and 120 lux on the closed arms. Testing consisted of 5min exploration time and was recorded using Ethovision XT. The time spent in the open and closed arms and the number of entries from the closed to the open arm was calculated.

Forced Swim Test: The Porsolt FST was conducted using a vertical clear glass cylinder (10 cm in diameter, 25 cm in height) filled with water (25°C). The mice spent 6 min in the water and immobility was scored from 2 to 6 min. Immobility was counted when the mouse floated motionless or made only those movements necessary to keep its head above the water.

Tail suspension test: The tails of the mice were wrapped with tape that covered approximately 4/5 of the tail length and then fixed upside down on a hook. The immobility time of each mouse was recorded and tracked over a 6 min period using Ethovision XT.

Locomotion: Locomotor activity was performed in 40 x 40 x 35 chambers (Stoelting Co, Wood Dale, IL) and distance traveled was recorded using Anymaze video-tracking software. All mice were handled and injected with saline (i.p) for 3 days to minimize stress. Mice were randomly

132 selected to be injected with saline or cocaine (i.p. 15mg/kg) and placed in the center of the
133 chambers. Distance traveled was measure for 3hr.

134 Condition Place Preference, Extinction and Reinstatement: Conditioned place preference (CPP)
135 was conducted using a two-chamber box with a tunnel adjoining the chambers with each
136 chamber distinguished by different color and floor textures (Stoelting Co, Wood Dale, IL). The
137 CPP procedure consisted of four phases: habituation, preconditioning test, conditioning and post-
138 conditioning test. On day 1 animals were habituated to the apparatus by allowing free access to
139 all compartments for 10 min. The following day all mice were exposed to 30 min
140 preconditioning phase, where each animal was given free access to the CPP apparatus to assess if
141 animals had a bias to a given side. Mice that spent <70% of the time in any of the two chambers
142 or tunnel were excluded from further evaluation. Subsequently, conditioning group (saline vs
143 cocaine) and drug-chamber pairings, were pseudo-randomly assigned to achieve a balanced CPP
144 design. During the 6 days of conditioning (Day 2-7), animals were injected once a day with
145 either vehicle or cocaine (4 or 10 mg/kg, i.p.) and immediately confined to one of the assigned
146 compartments for 30 min. The order of the drug administration was counterbalanced such that
147 half the animals received cocaine on the first day of conditioning and the other half on the
148 second day of conditioning. On day 8, mice were placed in the center of the tunnel and allowed
149 free access to all compartments for 30 min (post-conditioning). Place preference score was
150 calculated for each mouse as the difference between postconditioning and preconditioning time
151 spent in drug-paired compartment. After conditioning, daily extinction training was conducted.
152 During the extinction sessions, mice were placed into the center compartment and once again
153 provided free access to side compartments for 30 min. Mice underwent daily extinction training
154 twice a day (morning and afternoon) until the preference for the cocaine paired compartment

155 were similar to the preconditioning scores. Extinction was achieved when during the post-
156 extinguished test, the average preference for the cocaine paired compartment minus the standard
157 error of the mean was below zero. Those mice that met the extinguished criteria underwent a
158 reinstatement session. Reinstatement was performed the day following extinction. For stress-
159 induced reinstatement mice were exposed to 6min FST followed by 20min recovery in a paper
160 towel-lined cage and then a 30min test in the CPP apparatus as above. For cocaine reinstatement,
161 mice were injected with cocaine (10mg/kg). Mice were then placed into the apparatus and
162 allowed free access for 30min. Reinstatement was defined according to the time spent in the
163 compartment previously paired with cocaine. Time spent in each chamber was measured during
164 each phase of the CPP using video tracking followed by the analysis by Anymaze Software
165 (Wood Dale, IL).

166

167 **Quantitative proteomics and analysis**

168 Ventral and dorsal striatum (V. Str and D. Str) for Rgs7 sKO and WT mice were homogenized
169 and lysed in 6M guanidine, 100mM HEPES, pH = 8.5 and prepared as previously described (He
170 et al., 2019). Each sample was heated to 95 °C for 3 min. The proteins were reduced at 5 mM
171 DTT for 20 mins and alkylated at 15mM iodoacetamide for 20 mins. The reaction was quenched
172 by adding DTT to 50mM and incubation for 15 mins. Next, the solution was then diluted to
173 50mM HEPES, 1.5M Guanidine. 1 µg of Lys-C protease (Pierce) was added to each sample and
174 incubated for 3 h at room temperature whilst vortexing. 2 µg of trypsin protease (Pierce) was
175 added next and samples were incubated overnight at 37 °C while vortexing. Following digestion,
176 the samples were acidified 0.5% TFA, bound to alkylated resin (Pierce C18 spin columns), and
177 washed with 5% acetonitrile, 0.5% TFA. Samples were eluted from resin with 80% acetonitrile,

178 0.5% formic acid buffer. Eluted samples were dried down using vacuum centrifugation, and
179 resuspended in 50mM HEPES. MicroBCA (Pierce) was used to determine peptide mass
180 concentration. 80 µg of each sample were aliquoted for TMT labeling with 0.4 mg of a
181 respective TMT label (Thermo Scientific). V. Str and D.Str samples were labeled as 5xCre-
182 (WT) and 5xCre+ (Rgs7 sKO). Labeling reaction took place for 1 h and 15 mins at room
183 temperature. Reaction was quenched by bringing sample solutions to 0.3% (v/v) hydroxylamine
184 and incubated for 15 min at room temperature. The ten samples for each brain region was then
185 combined at a ratio of 1:1:1:1:1:1:1:1:1:1. The combined samples were then acidified to 0.5%
186 TFA, bound to alkylated resin (HyperSep C18 vacuum cartridges), and washed with 5%
187 acetonitrile, 0.5% TFA before being eluted with 80% acetonitrile, 0.5% formic acid. Eluted
188 combinatory samples were dried down using vacuum centrifugation, and subsequently
189 resuspended in 0.1% TFA. Samples were fractionated using strong cation exchange
190 nitrocellulose spin columns (Pierce). Six elution fractions for each sample were created
191 corresponding to 50mM sodium acetate (NaAcO), 100mM NaAcO, 250mM NaAcO, 500mM
192 NaAcO, 1M NaAcO, and 4M NaAcO. Every fraction was desalted by acidification to pH = 2
193 with TFA, binding to alkylated resin (Pierce C18 spin columns), washing with 5% acetonitrile,
194 0.5% TFA and eluted with 80% acetonitrile, 0.5% formic acid. Fractions were dried using
195 vacuum centrifugation, and resuspended in LCMS Buffer A: 5% acetonitrile, 0.125% formic
196 acid. Fractions were quantified using microBCA (Pierce). 3 µg from each fraction were loaded
197 for LC-MS analysis using a Thermo Orbitrap Fusion coupled to a Thermo EASY nLC-1200
198 UPLC pump and vented Acclaim Pepmap 100, 75 µm × 2 cm nanoViper trap column and
199 nanoViper analytical column: Thermo—164570, 3 µm, 100 Å, C18, 0.075 mm, 500 mm with
200 stainless steel emitter tip assembled on the Nanospray Flex Ion Source with a spray voltage of

201 2000V. For the chromatographic run, Buffer A contained (as above) and Buffer B contained 95%
202 acetonitrile, 0.125% formic acid. A four-hour gradient was established beginning with 100% A,
203 0% B and increased to 7% B over 5 mins, then to 25% B over 160 mins, 36% B over 40 mins,
204 45% B over 10 mins, 95% B over 10 mins, and held at 95% B for 15 mins before terminating the
205 scan. The multinotch MS3 method (McAlister et al., 2014) parameters include: Ion transfer tube
206 temp = 300 °C, Easy-IC internal mass calibration, default charge state = 2 and cycle time = 3 s.
207 MS1 detector set to orbitrap with 60 K resolution, wide quad isolation, mass range = normal,
208 scan range = 300–1800 m/z, max injection time = 50 ms, AGC target = 2×10^5 , microscans = 1,
209 RF lens = 60%, without source fragmentation, and datatype = positive and centroid. MIPS was
210 set as on, included charge states 2–7 and reject unassigned. Dynamic exclusion was enabled with
211 n = 1 exclusion for 60 s with 10ppm tolerance for high and low. An intensity threshold was set to
212 5×10^3 . Precursor selection decision = most intense, top speed, 3 s. MS2 settings include
213 isolation window = 0.7, scan range = auto normal, collision energy = 35% CID, scan rate =
214 turbo, max injection time = 50 ms, AGC target = 1×10^4 , Q = 0.25. The top ten precursors were
215 selected for MS3 analysis. Precursors were fragmented using 65% HCD before orbitrap
216 detection. A precursor selection range of 400–1200 m/z was chosen with mass range tolerance.
217 An exclusion mass width was set to 18 ppm on the low and 5 ppm on the high. Isobaric tag loss
218 exclusion was set to TMT reagent. Additional MS3 settings include an isolation window = 2,
219 orbitrap resolution = 60 K, scan range = 120 – 500 m/z, AGC target = 1×10^4 , max injection time
220 = 120 ms, microscans = 1, and datatype = profile. Spectral raw files were extracted into MS1,
221 MS2, and MS3 files using the in-house program RawConverter (He et al., 2015). Spectral files
222 were pooled from fractions and an unfractionated portion for each sample and searched against
223 the Uniprot mouse protein database (reviewed_iso_- cont_3_25_14) and matched to sequences

224 using the Pro- LuCID/SEQUEST algorithm (ProLuCID ver. 3.1) with 50 p.p.m. peptide mass
 225 tolerance for precursor ions and 600 p.p.m. for fragment ions. The search space included all fully
 226 and half-tryptic peptide candidates that fell within the mass tolerance window with no
 227 miscleavage constraint, assembled and filtered with DTASelect2 (ver. 2.1.3) through the
 228 Integrated Proteomics Pipeline (IP2 v.5.0.1, Integrated Proteomics Applications, Inc., CA, USA).
 229 Static modifications included 57.02146 C and 229.162932 K and N-term. Peptide probabilities
 230 and false discovery ratios were produced using a target/decoy approach. Each protein identified
 231 was required to have a minimum of one peptide of minimal length five. A false discovery rate of
 232 1% at the protein level was used for data filtering. Isobaric labeling analysis was performed with
 233 Census 2 as previously described (Park et al., 2014a). TMT channels were normalized by
 234 dividing it over the sum of all channels. No intensity threshold was applied.
 235 To calculate the fold change between Rgs7 sKO and WT, the average intensity values for each
 236 protein in the dataset were used and the values were standardized to the mean of the WT samples
 237 (n=5). The fold change was used to calculate the mean of the Rgs7 sKO standardized values and
 238 the p values were calculated by a Student's t-test. For Panther analysis, the list of significantly
 239 changed proteins were queried against all proteins in the both the ventral and dorsal striatum
 240 dataset using a statistical overrepresentation test of the GO biological process complete
 241 annotation (Mi et al., 2016).

242 **Western Blots**

243 Brains were quickly removed from euthanized Rgs7 sKO and WT mice and striatal tissue was
 244 lysed in ice-cold lysis buffer (300mM NaCl, 50mM Tris-HCl, pH 7.4, 1% Triton X-100, and
 245 complete protease inhibitor cocktail (Roche Applied Science, Penzberg, Germany) and
 246 phosphatase inhibitor mix (Sigma-Aldrich, St. Louis, MO)) and sonicated. Protein concentrations

247 was obtained using Pierce 660nm Protein Assay (Thermo Fisher, Waltham, MA). Samples were
 248 diluted in 4× SDS sample buffer, resolved by SDS-polyacrylamide gel electrophoresis (SDS-
 249 PAGE) and then transferred onto a PDVF membrane. Primary antibodies for anti-RGS7 and
 250 anti-GAPDH (Millipore) were detected by using HRP-conjugated secondary antibodies and ECL
 251 chemiluminescence system (Pierce, Rockford, IL). Signals were captured on film and scanned by
 252 densitometer, and band intensities were determined by using NIH ImageJ software.

253 **Quantification and statistical analysis**

254 Statistical analysis was performed using GraphPad Prism (Prism6.0, GraphPad, San Diego,
 255 California). Student's t test was used to compare means between two groups, and one-way or
 256 two-way analysis of variance followed by Tukey's or Bonferroni post hoc tests were used to
 257 determine significant differences among multiple groups. Differences were considered
 258 significant if $p < 0.05$. All data are expressed as means \pm SEM.

260 **RESULTS**

261 **Loss of Rgs7 in the striatum induces an antidepressant-like phenotype**

262 To study the role of striatal RGS7 in depression-related behaviors we eliminated Rgs7 in
 263 striatum by crossing conditional $Rgs7^{flx/flx}$ strain with a striatal specific driver $Rgs9^{cre}$ mice to
 264 generate $Rgs7^{flx/flx}Rgs9^{cre}$ (Rgs7 sKO) and their wildtype littermates, $Rgs7^{flx/flx}$ (WT) (Fig 1A).
 265 Mice were evaluated in a panel of behavioral tests to assess several aspects of anxiety-like and
 266 depressive-like behaviors including marble burying, elevated plus maze (EPM), tail suspension
 267 test (TST) and forced swim test (FST) (Fig 1B). In the marble burying test, Rgs7 sKO mice
 268 displayed an anxiolytic-like phenotype as evident by burying fewer marbles ($t_{(18)} = 2.999$, $p =$
 269 0.0077 , $n=10/genotype$) (Fig 1C). In the EPM, Rgs7 sKO mice spent more time in the open arm
 270 ($t_{(18)} = 2.802$, $p = 0.018$, $n=10/genotype$) and increased number of crossovers into the open arm

271 ($t_{(18)} = 2.999$, $p < 0.05$, $n=10/\text{genotype}$) (Figure 1D). Rgs7 sKO mice also exhibited a reduced
 272 immobility time in the tail suspension test (TST, $t_{(18)} = 2.637$, $p = 0.017$, $n=10/\text{genotype}$) (Fig
 273 1E). This antidepressant-like phenotype in the Rgs7 sKO mice was recapitulated in the forced
 274 swim test with a lower immobility time (FST, $t_{(18)} = 4.993$, $p = 0 < 0.0001$, $n=10/\text{genotype}$) and a
 275 higher swim (mobility) time ($t_{(18)} = 4.99$, $p = 0 < 0.0001$, $n=10/\text{genotype}$) (Fig 1F). In summary,
 276 the loss of striatal RGS7 induces an anxiolytic- and antidepressant-like phenotype.

277 To address the behavioral selectivity of Rgs7, we evaluated the role of Rgs9, a related
 278 member of the R7 RGS family, highly enriched in the striatum. In the marble burying test, there
 279 was no difference in the number of marbles buried between Rgs9 KO and their WT littermates
 280 (Fig 2A). There was no difference in time spent in the open arm of the EPM but the number of
 281 crosses were decreased in the Rgs9 KO mice ($t_{(18)} = 2.426$, $p < 0.05$, WT $n=9$ KO $n=11$) (Fig
 282 2B). Immobility times in the TST (Fig 2C) and FST (Fig 2D) were similar between Rgs9 KO
 283 and WT mice. Thus, loss of Rgs7, but not Rgs9 in the striatum, selectively affects depression-
 284 related behaviors.

285 **Ablation of striatal Rgs7 does not influence behavioral responses to cocaine**

286 Previous studies implicated striatal Rgs7 in regulating the behavioral responses to
 287 morphine (Sutton et al., 2016). In order to determine whether this effect reflected general
 288 changes in reward setpoint common across drugs of abuse, we assessed the effects of cocaine
 289 administration in our Rgs7 sKO. In an open field arena, both WT and Rgs7 sKO mice showed
 290 increase in locomotor activity to cocaine as compared with saline (treatment $F_{1,44} = 11.08$, $p =$
 291 0.018 , $n=12/\text{genotype}$) (Fig 3A). No significant difference between the genotypes was observed
 292 following cocaine administration. Locomotor activity was also examined following daily 5 days
 293 of cocaine administration and no difference between genotypes were found (Fig 3B).

294 To test the rewarding effects of cocaine, CPP was conducted at doses of 4 and 10 mg/kg
 295 (Fig 3C). As expected, cocaine administration induced a place preference at both doses that was
 296 observed by an increase in the time spent in the drug-paired compartment during the
 297 postconditioning phase compared with the pre-conditioning phase (Fig 3D; treatment $F_{2,39} =$
 298 23.85, $p < 0.0001$, $n=6-12/\text{genotype}$). We found no significant difference in the place preference
 299 score between genotypes at either cocaine dose. Collectively, these results show that Rgs7
 300 deficiency in striatal neurons does not alter cocaine- induced psychomotor activation,
 301 sensitization, or the rewarding properties of the drug.

302

303 **Elimination of striatal Rgs7 abolishes stress-induced reinstatement**

304 Stress is a major factor influencing drug-seeking behaviors and as such we investigated
 305 the role of RGS7 in a stress-reinstatement of cocaine CPP (Fig 4A). A 10 mg/kg cocaine dose
 306 was chosen to assess the role of RGS7 in stress-induced reinstatement. The place preference for
 307 cocaine was extinguished following six days of drug-free sessions where the time mice spent in
 308 the drug-paired compartment was similar between the post-extinguished phase and the
 309 preconditioned phase (Fig 4B; time $F_{6,66} = 5.489$, $p = 0.0001$, WT $n=5$, KO $n=8$). There was no
 310 difference between genotypes in the number of days to extinguish the place preference. To
 311 induce cocaine-reinstatement mice were subjected to a priming dose of cocaine or saline.
 312 Following the extinction of CPP, both WT and Rgs7 sKO mice were reinstated with cocaine and
 313 no difference between genotype was observed (Fig. 4C; treatment $F_{2,22} = 10.78$, $p = 0.0005$, WT
 314 $n=5$, KO $n=8$). There was no change in the place preference score with saline injection. A
 315 separate cohort of mice underwent extinction for cocaine CPP (Fig 4D; time $F_{6,72} = 7.246$, p
 316 0.0001 WT $n=6$ KO $n=8$) and then were subjected to an acute stressor, a forced swim. The force

317 swim stressor induced a place preference in WT but not in Rgs7 sKO mice (Fig 4E; genotype
318 $F_{1,12} = 6.585$, $p < 0.01$, treatment $F_{1,12} = 12.06$, $p = 0.0046$, interaction $F_{1,12} = 9.745$, $p = 0.0088$,
319 WT $n=6$, KO $n=8$). Thus, loss of Rgs7 selectively protects mice from forced swim stress but not
320 drug induced reinstatement of cocaine CPP.

321

322 **Effects of Rgs7 elimination on the proteome**

323 To obtain insights into possible molecular underpinnings associated with the effect of striatal
324 Rgs7 on behavior we identified proteins whose expression in the striatum was affected by the
325 loss of Rgs7. This was achieved by carrying out a quantitative mass spectrometry of proteins in
326 both the dorsal and ventral striatum. We found that 42 of 491 proteins in the ventral (Fig 5A) and
327 23 of 885 proteins in the dorsal striatum (Fig 5B) were significantly differentially expressed
328 between WT and Rgs7 sKO mice (p values in the range 0.0499 to 6.9×10^{-4} , Student's t -test,
329 $n=5$ /genotype, Extended Data Figure 5-1). To obtain insight into the processes affected by these
330 changes we explored association of proteins with significantly altered expression with functional
331 networks using the Panther classification system. This analysis revealed that loss of striatal Rgs7
332 had a major effect on initiation of translation, vesicle fusion and synaptic vesicle exocytosis (Fig
333 5C). In particular, components of the eukaryotic initiation factor (eIF) complex, a cascade that
334 regulates the initiation step in mRNA translation (Sonenberg and Hinnebusch, 2009) were
335 differentially expressed in both regions of the striatum (Fig 5A and 5B). Based on these results,
336 we conclude that Rgs7 may exert many of its effects by controlling GPCR effects on protein
337 biosynthesis and synaptic communication.

338

339

340 DISCUSSION

341 The current study demonstrates the contribution of striatal Rgs7 towards depression-related
342 behaviors and their relevance to substance abuse. Our behavioral experiments show that the lack
343 of RGS7 in the striatum results in an antidepressant-like and anxiolytic-like phenotype but does
344 not affect cocaine-induced locomotion, sensitization or CPP. Furthermore, striatal specific
345 ablation of Rgs7 resulted in a resiliency to stress reinstatement of previously extinguished
346 cocaine CPP but not following re-exposure to a priming dose of the cocaine. We also found that
347 elimination of Rgs9, a highly related and abundant RGS protein in the same neuronal
348 populations produced no behavioral effects in the depressive-like assays. These observations
349 suggest that the reactions that lead to the development of the phenotype are specifically
350 controlled by the Rgs7. Overall, the results reveal a prominent contribution of striatal neurons
351 controlled by Rgs7 to depressive-like behaviors and stress-induced reinstatement.

352 We have previously found that the elimination of Rgs7 in the PFC was sufficient to drive
353 antidepressant-like and anxiolytic-like phenotype using the same behavioral tests (Orlandi et al.,
354 2019). Current results complement these findings and demonstrate the ability of Rgs7 to act
355 across different brain circuits to regulate affective behaviors. Perhaps it is not entirely surprising
356 that our results revealed no regional specificity of Rgs7 effects as both the PFC and striatum are
357 interconnected and involved in mediating mood and emotionality. While the exact molecular
358 mechanism underlying the observed behavioral effects remains to be determined, it is known that
359 Rgs7 acts as a negative regulation of G α i/o-coupled GPCRs (Anderson et al., 2009b). Studies
360 with a global knockout of Rgs7, implicated both of α 2A-adrenergic and GABAB receptors as
361 mediators of antidepressant phenotypes (Orlandi et al., 2019). This suggests that multiple GPCRs

362 may play a role in this process and it would be of interest to explore which GPCR system drives
363 the striatal phenotype.

364 Given that RGS proteins are direct regulators of GPCR signaling, there has been a
365 forthcoming effort to study their role in the etiology and treatment of depression (Senese et al.,
366 2018) and our study adds to this knowledge. Our genetic manipulations allow for a direct
367 comparison of Rgs7 and Rgs9 in the same neuronal population allowing us to conclude that they
368 have distinct behavioral profiles within the striatum and do not compensate for each other. The
369 other brain-enriched member of the R7 family, Rgs6 has also been implicated in mood
370 regulation. Global Rgs6 knockout mice display antidepressant-like behaviors and this phenotype
371 was reversed by serotonin 5-HT_{1A} receptor antagonist pretreatment (Stewart et al., 2014).
372 However, treatment with 5-HT_{1A} antagonist has been shown to be ineffective towards the
373 antidepressant-like phenotype in a model of Rgs7 (Orlandi et al., 2019). Even though these
374 members of the R7 family all target G α i/o (Posner et al., 1999; Hooks et al., 2003), share
375 common binding partners (Cabrera et al., 1998; Makino et al., 1999; Zhang and Simonds, 2000;
376 Martemyanov et al., 2005) and are expressed in the striatum (Thomas et al., 1998; Rahman et al.,
377 1999; Anderson et al., 2009a), there appears to be a selectivity for the G α i/o coupled GPCR and
378 consequently produces different phenotypic outcomes (Anderson et al., 2009b). This
379 nonredundant function of RGS-mediated behaviors has been observed in other behavioral
380 paradigms and it is intriguing how selective Rgs7 is towards Gi/o-coupled GPCR signaling
381 (Zachariou et al., 2003; Anderson et al., 2010; Sutton et al., 2016). Furthermore, it appears that
382 the loss of one R7 member is not compensated by other members of the family, even though they
383 are all expressed in the same striatal neurons. In agreement with this, the elimination of Rgs7

384 does not affect the levels of Rgs6 or Rgs9 and thus we attribute our observed behavioral effects
385 to the loss of Rgs7 expression (Sutton et al., 2016).

386 In this study, the driver line Rgs9^{cre} was utilized to target striatal neurons, as expression
387 of Cre recombinase has been shown to be restricted to postsynaptic neurons in the striatum
388 (Sutton et al., 2016; Tecuapetla et al., 2016). Western blots showed a substantial decrease of
389 striatal Rgs7 protein with residual amounts likely from glial cells that do not express Cre and/or
390 from incoming projection from the VTA, cortex and other brain regions (Dang et al., 2006).
391 Furthermore, this knockout strategy does not discriminate between medium spiny neurons and
392 cholinergic interneurons. As Rgs7 is expressed in these neuronal populations, we cannot fully
393 address the cell-specific contributions of Rgs7 towards depression-like behaviors. While future
394 studies are needed to parse out the cell-specific roles of Rgs7 in the striatum, it appears striatal
395 Rgs7 is a molecular determinant to drive stress-related behaviors.

396 The behavioral paradigm to assess depressive-like behaviors allowed us to evaluate an
397 individual animal across complementary tests (MB, EPM, TST and FST). This multimodal
398 approach has been shown to reduce behavioral variability across several tests and allow for a
399 robust and comprehensive characterization for an individual mouse (Crawley and Paylor, 1997;
400 Guilloux et al., 2011). Although the order across multiple days of testing is designed to mitigated
401 stress (least to the more stressful test) we cannot rule out that conducting several tests could
402 influence behavioral outcomes.

403 Stress and drug re-exposure are common precipitating factors for relapse in recovering
404 cocaine addicts. Although both stimuli can trigger drug relapse, they do not necessarily require
405 activation of overlapping neurobiological pathways (Kalivas and McFarland, 2003). Significant
406 effort has been made to dissect the mechanism involved in stress and drug cued relapse. For

407 example, metabotropic glutamate receptors have been implicated in cocaine priming and
408 reinstatement (Baker et al., 2003; Kupchik et al., 2012), where both mGluR2/3 and mGluR5
409 inhibition in the NAc have been shown to prevent cocaine reinstatement (Kumaresan et al., 2009;
410 Mahler et al., 2014). Targeting CREB signaling in the NAc affected stress reinstatement but
411 failed to augment drug induced reinstatement (Kreibich and Blendy, 2004; Briand et al., 2010).
412 CREB is activated by the cAMP pathway and we have found that Rgs7 KO mice have an
413 increase in cAMP levels (Orlandi et al., 2019). Our findings that Rgs7 is a mediator of stress
414 reinstatement but not for cocaine agree with previous studies that have demonstrated dissociable
415 mechanisms of pharmacological and stress reinstatement (Mantsch et al., 2010; Nair et al.,
416 2013). In addition to Rgs7 being a mediator of stress reinstatement, it also prevents stress-
417 induced depression (Orlandi et al., 2019). This raises an intriguing notion that Rgs7 may be a
418 general regulator for stress-related behaviors.

419 Our results also provide interesting insights into changes in striatal proteome induced by
420 the loss of Rgs7. Notably, our proteomic screen revealed several eukaryotic initiation factors
421 (eIF) that were significantly differential expressed in striatal tissues lacking Rgs7. The eIF
422 complex is considered to be the rate limiting step in protein synthesis tightly regulating this
423 fundamental cellular process (Sonenberg and Hinnebusch, 2009). A growing body of evidence
424 has implicated the importance of eIF in normal neuronal cell function (Amorim et al., 2018).
425 Inhibition of this process induces depressive-like behaviors in rodents, and downregulation of
426 several eIF proteins have been detected in MDD patients (Jernigan et al., 2011; Yang et al.,
427 2013; Aguilar-Valles et al., 2018). Furthermore, ketamine and traditional antidepressants affect
428 local protein synthesis and this action is sufficient to ameliorate depressive-like behaviors (Park

429 et al., 2014b; Liu et al., 2015). While further investigation of Rgs7 signaling is warranted, it is
430 plausible that Rgs7 influence on protein synthesis drives depressive-like responses.

431 In summary, our data demonstrates that Rgs7 plays a prominent role in depression and
432 the regulation of stress-induced reinstatement of cocaine CPP. Together these finding may
433 provide a better understanding for the molecular mechanism involved in resiliency to the
434 maladaptive effects of stress.

435

436 **FIGURE LEGENDS**

437 Figure 1: Ablation of striatal Rgs7 in mice results in an antidepressant-like phenotype. A)
438 Representative western blots and graphs of densitometry values for Rgs7 levels in the striatum of
439 WT and Rgs7 sKO mice (n=4/genotype). B) Scheme of behavioral tests. WT and Rgs7 sKO
440 mice were tested in C) marble burying, D) elevated plus maze, E) tail suspension test (TST) and
441 F) forced swim test (FST, n=10/genotype). Data shown as means \pm SEM (*p<0.05, **p<0.01,
442 ***p<0.001).

443
444 Figure 2: Elimination of Rgs9 does not influence behavior in acute stress procedures.
445 Rgs9 knockout mice were tested in A) marble burying, B) elevated plus maze, C) tail suspension
446 test (TST) and D) forced swim test (FST, n=9-11 genotype). Data shown as means \pm SEM
447 (*p<0.05).

448
449 Figure 3: Elimination of striatal Rgs7 in mice does not affect cocaine-induced locomotion or
450 CPP. A) Total distance traveled for mice injected with saline or cocaine (15mg/kg). B) Total
451 distance traveled for mice injected daily with cocaine for 5 days (n=12mice/genotype). C)
452 Timeline for CPP. D) Effects of cocaine-induced CPP at doses of 4mg/kg and 10mg/kg (n=6-
453 11/genotype). Place preference scores are calculated as the difference between time spent in the
454 drug-paired side during postconditioning vs. preconditioning tests. Data shown as means \pm SEM.

455 Figure 4: Ablation of striatal Rgs7 in mice display resiliency to stress-induced reinstatement A)
456 Timeline for reinstatement. B) Time course for extinction of cocaine CPP (n=5-8mice/genotype).
457 C) Cocaine reinstatement of extinguished cocaine-induced CPP (n=5-8mice/genotype). D) Time
458 course for extinction of cocaine CPP (n=6-8mice/genotype). E) Force swim test reinstatement of
459 extinguished cocaine-induced CPP. Data shown as means \pm SEM (*p<0.05, ***p<0.001).

460 Figure 5: Proteomic analysis from conditional Rgs7 knockout mice. Volcano plot showing the
461 protein level fold change relative to significance between WT and Rgs7 sKO mice in the A)
462 dorsal and B) ventral striatum. Significantly upregulated proteins are in blue (p value < 0.05),
463 significantly downregulated proteins are in red (p value < 0.05), and all other proteins are in
464 black (n =5/genotype). Comparison of fold differences for all quantified proteins found in
465 Extended Data Figure 5-1. C) Panther analysis of statistically overrepresented biological
466 processes in the ventral and dorsal striatum of Rgs7 sKO mice. Dotted line indicates Bonferroni
467 corrected p value = 0.05). Shown as a rank ordered list of most significant general biological
468 processes.

471 **EXTENDED FIGURE LEGEND**

472 Extended Data Figure 5-1: Fold differences between WT and Rgs7 sKO mice for the proteomic
473 analysis. Table listing all quantified proteins between WT and Rgs7 sKO mice in the dorsal and
474 ventral striatum. Columns are arranged left-to-right as protein accession number, gene name,
475 fold change (KO vs. WT), Log₂ of fold change, Student's t-test, -Log₁₀ of t-test, and protein
476 description. Log₂ fold change and -Log₁₀ t-test are the values graphed in the volcano plots of fig
477 5A and 5B.

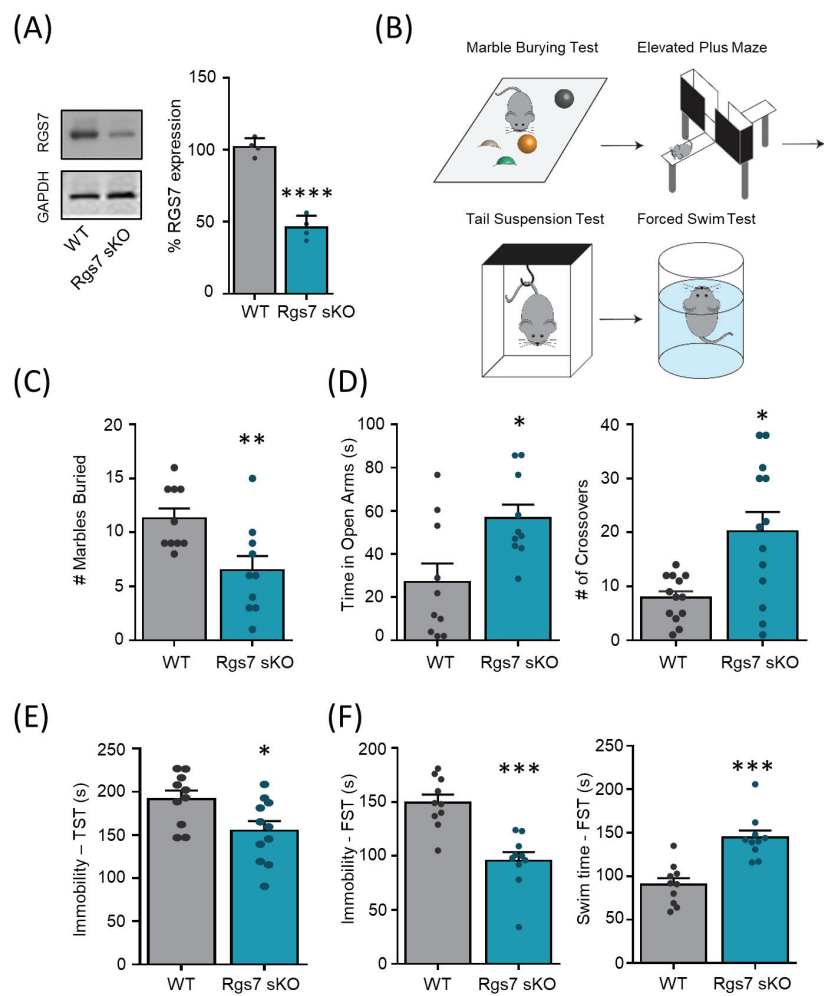
REFERENCES

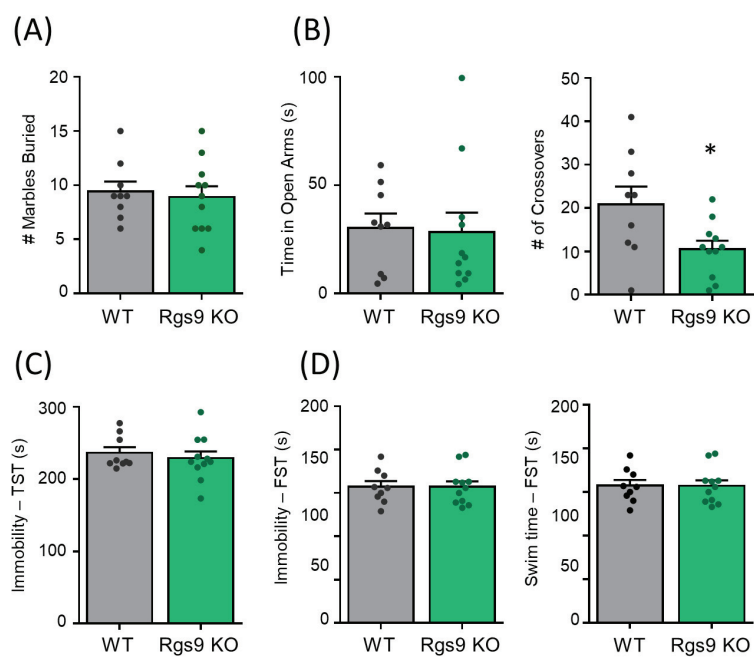
- Aguilar-Valles A, Haji N, De Gregorio D, Matta-Camacho E, Eslamizade MJ, Popic J, Sharma V, Cao R, Rummel C, Tanti A, Wiebe S, Nunez N, Comai S, Nadon R, Luheshi G, Mechawar N, Turecki G, Lacaille JC, Gobbi G, Sonenberg N (2018) Translational control of depression-like behavior via phosphorylation of eukaryotic translation initiation factor 4E. *Nat Commun* 9:2459.
- Amorim IS, Lach G, Gkogkas CG (2018) The Role of the Eukaryotic Translation Initiation Factor 4E (eIF4E) in Neuropsychiatric Disorders. *Front Genet* 9:561.
- Anderson GR, Lujan R, Martemyanov KA (2009a) Changes in striatal signaling induce remodeling of RGS complexes containing Gbeta5 and R7BP subunits. *Mol Cell Biol* 29:3033-3044.
- Anderson GR, Posokhova E, Martemyanov KA (2009b) The R7 RGS protein family: multi-subunit regulators of neuronal G protein signaling. *Cell Biochem Biophys* 54:33-46.
- Anderson GR, Cao Y, Davidson S, Truong HV, Pravetoni M, Thomas MJ, Wickman K, Giesler GJ, Jr., Martemyanov KA (2010) R7BP complexes with RGS9-2 and RGS7 in the striatum differentially control motor learning and locomotor responses to cocaine. *Neuropsychopharmacology* 35:1040-1050.
- Baker DA, McFarland K, Lake RW, Shen H, Tang XC, Toda S, Kalivas PW (2003) Neuroadaptations in cystine-glutamate exchange underlie cocaine relapse. *Nat Neurosci* 6:743-749.
- Berton O, McClung CA, Dileone RJ, Krishnan V, Renthal W, Russo SJ, Graham D, Tsankova NM, Bolanos CA, Rios M, Monteggia LM, Self DW, Nestler EJ (2006) Essential role of BDNF in the mesolimbic dopamine pathway in social defeat stress. *Science* 311:864-868.
- Briand LA, Vassoler FM, Pierce RC, Valentino RJ, Blendy JA (2010) Ventral tegmental afferents in stress-induced reinstatement: the role of cAMP response element-binding protein. *J Neurosci* 30:16149-16159.
- Cabrera JL, de Freitas F, Satpaev DK, Slepak VZ (1998) Identification of the Gbeta5-RGS7 protein complex in the retina. *Biochem Biophys Res Commun* 249:898-902.
- Cao Y, Pahlberg J, Sarria I, Kamasawa N, Sampath AP, Martemyanov KA (2012) Regulators of G protein signaling RGS7 and RGS11 determine the onset of the light response in ON bipolar neurons. *Proc Natl Acad Sci U S A* 109:7905-7910.
- Cerovic M, d'Isa R, Tonini R, Brambilla R (2013) Molecular and cellular mechanisms of dopamine-mediated behavioral plasticity in the striatum. *Neurobiol Learn Mem* 105:63-80.
- Crawley JN, Paylor R (1997) A proposed test battery and constellations of specific behavioral paradigms to investigate the behavioral phenotypes of transgenic and knockout mice. *Horm Behav* 31:197-211.
- Dang MT, Yokoi F, Yin HH, Lovinger DM, Wang Y, Li Y (2006) Disrupted motor learning and long-term synaptic plasticity in mice lacking NMDAR1 in the striatum. *Proc Natl Acad Sci U S A* 103:15254-15259.
- Francis TC, Lobo MK (2017) Emerging Role for Nucleus Accumbens Medium Spiny Neuron Subtypes in Depression. *Biol Psychiatry* 81:645-653.
- Guilloux JP, Seney M, Edgar N, Sibille E (2011) Integrated behavioral z-scoring increases the sensitivity and reliability of behavioral phenotyping in mice: relevance to emotionality and sex. *J Neurosci Methods* 197:21-31.
- He L, Diedrich J, Chu YY, Yates JR (2015) Extracting Accurate Precursor Information for Tandem Mass Spectra by RawConverter. *Anal Chem* 87:11361-11367.
- He Q, Arroyo ED, Smukowski SN, Xu J, Piochon C, Savas JN, Portera-Cailliau C, Contractor A (2019) Critical period inhibition of NKCC1 rectifies synapse plasticity in the somatosensory cortex and restores adult tactile response maps in fragile X mice. *Mol Psychiatry* 24:1732-1747.

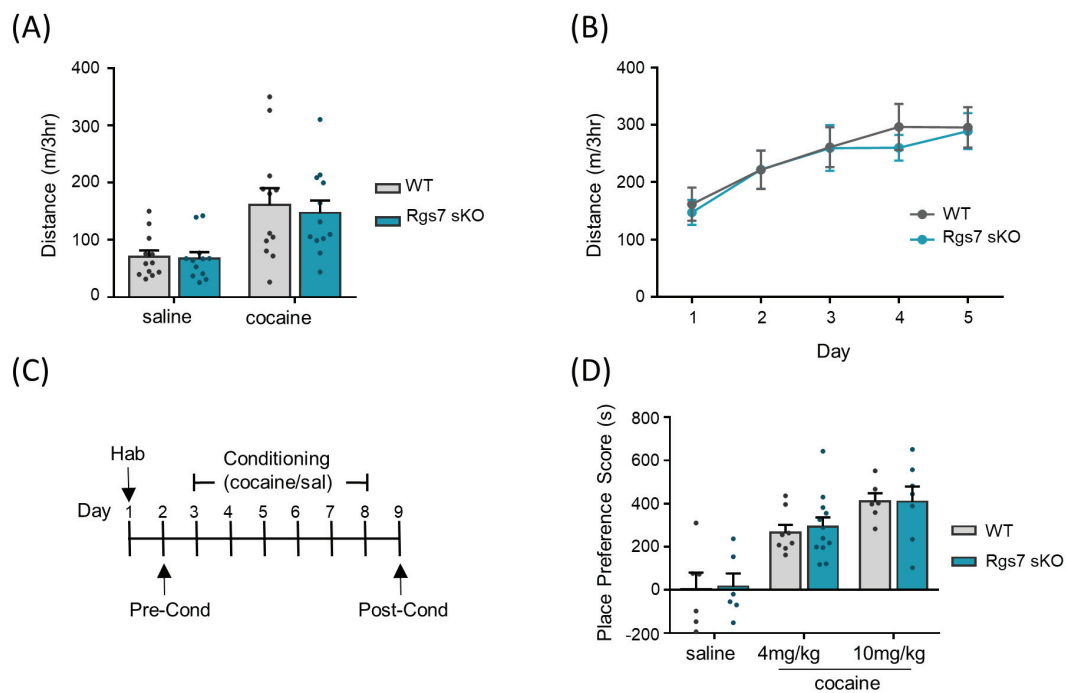
- 526 Hollinger S, Hepler JR (2002) Cellular regulation of RGS proteins: modulators and integrators of G protein
527 signaling. *Pharmacol Rev* 54:527-559.
- 528 Hooks SB, Waldo GL, Corbitt J, Bodor ET, Krumins AM, Harden TK (2003) RGS6, RGS7, RGS9, and RGS11
529 stimulate GTPase activity of Gi family G-proteins with differential selectivity and maximal
530 activity. *J Biol Chem* 278:10087-10093.
- 531 Jernigan CS, Goswami DB, Austin MC, Iyo AH, Chandran A, Stockmeier CA, Karolewicz B (2011) The
532 mTOR signaling pathway in the prefrontal cortex is compromised in major depressive disorder.
533 *Prog Neuropsychopharmacol Biol Psychiatry* 35:1774-1779.
- 534 Johnson KA, Lovinger DM (2016) Presynaptic G Protein-Coupled Receptors: Gatekeepers of Addiction?
535 *Front Cell Neurosci* 10:264.
- 536 Kalivas PW, McFarland K (2003) Brain circuitry and the reinstatement of cocaine-seeking behavior.
537 *Psychopharmacology (Berl)* 168:44-56.
- 538 Kreibich AS, Blendy JA (2004) cAMP response element-binding protein is required for stress but not
539 cocaine-induced reinstatement. *J Neurosci* 24:6686-6692.
- 540 Kreitzer AC (2009) Physiology and pharmacology of striatal neurons. *Annu Rev Neurosci* 32:127-147.
- 541 Kumaresan V, Yuan M, Yee J, Famous KR, Anderson SM, Schmidt HD, Pierce RC (2009) Metabotropic
542 glutamate receptor 5 (mGluR5) antagonists attenuate cocaine priming- and cue-induced
543 reinstatement of cocaine seeking. *Behav Brain Res* 202:238-244.
- 544 Kupchik YM, Moussawi K, Tang XC, Wang X, Kalivas BC, Kolokithas R, Ogburn KB, Kalivas PW (2012) The
545 effect of N-acetylcysteine in the nucleus accumbens on neurotransmission and relapse to
546 cocaine. *Biol Psychiatry* 71:978-986.
- 547 Liu XL, Luo L, Mu RH, Liu BB, Geng D, Liu Q, Yi LT (2015) Fluoxetine regulates mTOR signalling in a region-
548 dependent manner in depression-like mice. *Sci Rep* 5:16024.
- 549 Lobo MK, Nestler EJ (2011) The striatal balancing act in drug addiction: distinct roles of direct and
550 indirect pathway medium spiny neurons. *Front Neuroanat* 5:41.
- 551 Mahler SV, Hensley-Simon M, Tahsili-Fahadan P, LaLumiere RT, Thomas C, Fallon RV, Kalivas PW, Aston-
552 Jones G (2014) Modafinil attenuates reinstatement of cocaine seeking: role for cystine-
553 glutamate exchange and metabotropic glutamate receptors. *Addict Biol* 19:49-60.
- 554 Makino ER, Handy JW, Li T, Arshavsky VY (1999) The GTPase activating factor for transducin in rod
555 photoreceptors is the complex between RGS9 and type 5 G protein beta subunit. *Proc Natl Acad*
556 *Sci U S A* 96:1947-1952.
- 557 Mantsch JR, Weyer A, Vranjkovic O, Beyer CE, Baker DA, Caretta H (2010) Involvement of noradrenergic
558 neurotransmission in the stress- but not cocaine-induced reinstatement of extinguished
559 cocaine-induced conditioned place preference in mice: role for beta-2 adrenergic receptors.
560 *Neuropsychopharmacology* 35:2165-2178.
- 561 Martemyanov KA, Yoo PJ, Skiba NP, Arshavsky VY (2005) R7BP, a novel neuronal protein interacting with
562 RGS proteins of the R7 family. *J Biol Chem* 280:5133-5136.
- 563 Masuho I, Xie K, Martemyanov KA (2013) Macromolecular composition dictates receptor and G protein
564 selectivity of regulator of G protein signaling (RGS) 7 and 9-2 protein complexes in living cells. *J*
565 *Biol Chem* 288:25129-25142.
- 566 McAlister GC, Nusinow DP, Jedrychowski MP, Wühr M, Huttlin EL, Erickson BK, Rad R, Haas W, Gygi SP
567 (2014) MultiNotch MS3 enables accurate, sensitive, and multiplexed detection of differential
568 expression across cancer cell line proteomes. *Anal Chem* 86:7150-7158.
- 569 Mi H, Poudel S, Muruganujan A, Casagrande JT, Thomas PD (2016) PANTHER version 10: expanded
570 protein families and functions, and analysis tools. *Nucleic Acids Res* 44:D336-342.
- 571 Nair SG, Furay AR, Liu Y, Neumaier JF (2013) Differential effect of viral overexpression of nucleus
572 accumbens shell 5-HT1B receptors on stress- and cocaine priming-induced reinstatement of
573 cocaine seeking. *Pharmacol Biochem Behav* 112:89-95.

- 574 Nelson AB, Kreitzer AC (2014) Reassessing models of basal ganglia function and dysfunction. *Annu Rev*
575 *Neurosci* 37:117-135.
- 576 Orlandi C, Sutton LP, Muntean BS, Song C, Martemyanov KA (2019) Homeostatic cAMP regulation by the
577 RGS7 complex controls depression-related behaviors. *Neuropsychopharmacology* 44:642-653.
- 578 Park SK, Aslanian A, McClatchy DB, Han X, Shah H, Singh M, Rauniyar N, Moresco JJ, Pinto AF, Diedrich
579 JK, Delahunty C, Yates JR (2014a) Census 2: isobaric labeling data analysis. *Bioinformatics*
580 30:2208-2209.
- 581 Park SW, Lee JG, Seo MK, Lee CH, Cho HY, Lee BJ, Seol W, Kim YH (2014b) Differential effects of
582 antidepressant drugs on mTOR signalling in rat hippocampal neurons. *Int J*
583 *Neuropsychopharmacol* 17:1831-1846.
- 584 Pettinati HM, O'Brien CP, Dundon WD (2013) Current status of co-occurring mood and substance use
585 disorders: a new therapeutic target. *Am J Psychiatry* 170:23-30.
- 586 Posner BA, Gilman AG, Harris BA (1999) Regulators of G protein signaling 6 and 7. Purification of
587 complexes with gbeta5 and assessment of their effects on g protein-mediated signaling
588 pathways. *J Biol Chem* 274:31087-31093.
- 589 Rahman Z, Gold SJ, Potenza MN, Cowan CW, Ni YG, He W, Wensel TG, Nestler EJ (1999) Cloning and
590 characterization of RGS9-2: a striatal-enriched alternatively spliced product of the RGS9 gene. *J*
591 *Neurosci* 19:2016-2026.
- 592 Ross EM, Wilkie TM (2000) GTPase-activating proteins for heterotrimeric G proteins: regulators of G
593 protein signaling (RGS) and RGS-like proteins. *Annu Rev Biochem* 69:795-827.
- 594 Senese NB, Rasenick MM, Traynor JR (2018) The Role of G-proteins and G-protein Regulating Proteins in
595 Depressive Disorders. *Front Pharmacol* 9:1289.
- 596 Sonenberg N, Hinnebusch AG (2009) Regulation of translation initiation in eukaryotes: mechanisms and
597 biological targets. *Cell* 136:731-745.
- 598 Stewart A, Maity B, Wunsch AM, Meng F, Wu Q, Wemmie JA, Fisher RA (2014) Regulator of G-protein
599 signaling 6 (RGS6) promotes anxiety and depression by attenuating serotonin-mediated
600 activation of the 5-HT(1A) receptor-adenylyl cyclase axis. *FASEB J* 28:1735-1744.
- 601 Sutton LP, Ostrovskaya O, Dao M, Xie K, Orlandi C, Smith R, Wee S, Martemyanov KA (2016) Regulator of
602 G-Protein Signaling 7 Regulates Reward Behavior by Controlling Opioid Signaling in the Striatum.
603 *Biol Psychiatry* 80:235-245.
- 604 Tecuapetla F, Jin X, Lima SQ, Costa RM (2016) Complementary Contributions of Striatal Projection
605 Pathways to Action Initiation and Execution. *Cell* 166:703-715.
- 606 Thomas EA, Danielson PE, Sutcliffe JG (1998) RGS9: a regulator of G-protein signalling with specific
607 expression in rat and mouse striatum. *J Neurosci Res* 52:118-124.
- 608 Witherow DS, Wang Q, Levay K, Cabrera JL, Chen J, Willars GB, Slepak VZ (2000) Complexes of the G
609 protein subunit gbeta 5 with the regulators of G protein signaling RGS7 and RGS9.
610 Characterization in native tissues and in transfected cells. *J Biol Chem* 275:24872-24880.
- 611 Yang C, Zhou ZQ, Gao ZQ, Shi JY, Yang JJ (2013) Acute increases in plasma mammalian target of
612 rapamycin, glycogen synthase kinase-3beta, and eukaryotic elongation factor 2 phosphorylation
613 after ketamine treatment in three depressed patients. *Biol Psychiatry* 73:e35-36.
- 614 Zachariou V, Georgescu D, Sanchez N, Rahman Z, DiLeone R, Berton O, Neve RL, Sim-Selley LJ, Selley DE,
615 Gold SJ, Nestler EJ (2003) Essential role for RGS9 in opiate action. *Proc Natl Acad Sci U S A*
616 100:13656-13661.
- 617 Zhang JH, Simonds WF (2000) Copurification of brain G-protein beta5 with RGS6 and RGS7. *J Neurosci*
618 20:RC59.

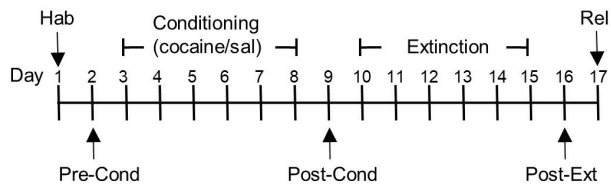
619



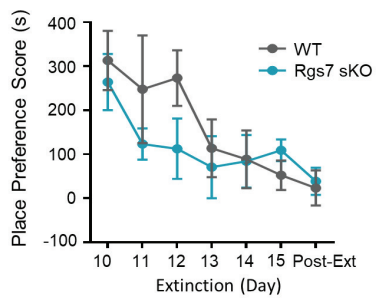




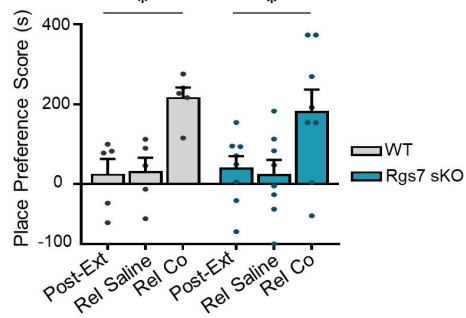
(A)



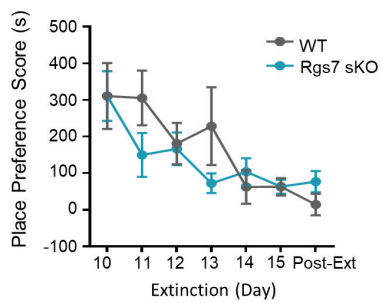
(B)



(C)



(D)



(E)

